

Topological energy braiding of the non-Bloch bands

Yang Li,¹ Xiang Ji,¹ Yuanping Chen,^{1,*} Xiaohong Yan,¹ and Xiaosen Yang^{1,†}

¹Department of Physics, Jiangsu University, Zhenjiang, 212013, China

(Dated: June 8, 2022)

The non-Hermitian skin effect, as a unique feature of non-Hermitian systems, will break the topological energy braiding of the Bloch bands in open boundary systems. Going beyond the Bloch band theory, we unveil the energy braiding of the non-Bloch bands by introducing a one-dimensional non-Hermitian tight-binding model. We find an entirely new generic class of topological non-Bloch bands such as Hopf link, which is generally generated by the non-Hermitian skin effect. The energy braiding is topologically robust against any perturbations without gap closing. Furthermore, non-Bloch topological invariants are proposed based on the generalized Brillouin zone to characterize the topology of these non-Bloch bands. The topological phase transition between the distinct phases occurs with the non-Bloch bands touching at exceptional points. We hope that our work can shed light on the topological energy braiding of the non-Bloch bands for non-Hermitian systems.

Non-Hermitian (NH) Hamiltonians [1–7], applicable to a wide range of open systems such as photonic[8–14], cold atomic [15–20], and acoustic [21–25] systems with gain/loss, have attracted immense growing interest, especially in the topological properties [26–30]. In contrast to Hermitian systems, NH systems have complex eigenenergies, which give rise to unique phenomena without Hermitian counterparts like the exceptional points (EPs) [31–38], non-Hermitian skin effect (NHSE) [6, 39–51], and non-Bloch bulk-boundary correspondence[52–63]. The NH systems can be described by generalizing the Brillouin zone(BZ) into a complex plane. For one-dimensional (1D) NH systems with a line or point gap [39] in the complex energy plane, the topologically distinct phases can be classified by the non-Bloch topological invariants defined on the generalized Brillouin zone (GBZ)[6, 52], for example, non-Bloch winding numbers[52, 64] and non-Bloch Chern numbers[65–67]. NHSE and non-Bloch topological invariants are of fundamental importance for understanding of topological phenomena in non-Hermitian systems.

Recent works show that the complex eigenenergies of the NH systems can form intricate band structures [68, 69]. The Bloch bands of the NH periodic boundary systems can separate from each other in momentum space. Then, the complex energies of the separable Bloch bands can braid topologically and correspond to the conjugacy classes of the braid group[70–72]. For the periodicity of the BZ, the knot invariants completely classify the separable Bloch bands for 1D NH periodic boundary systems[73, 74]. However, these topological invariants defined on BZ can not characterize the topological properties of the NH open boundary systems. In the presence of NHSE, the complex eigenenergies will collapse, which completely devastated the topological energy braiding of Bloch bands in the momentum space. Therefore, is there any non-Bloch bands with topological energy braiding? How to characterize the topological properties of the non-Bloch bands?

In this paper, we investigate the topological energy

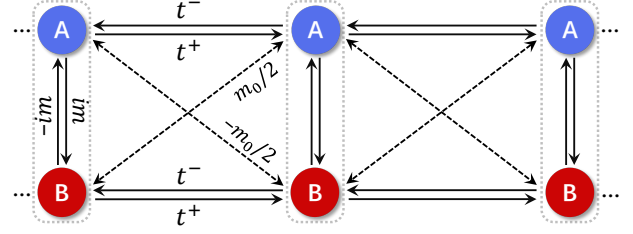


FIG. 1. Sketch of the two bands non-Hermitian lattice model with non-reciprocal nearest-neighbour hopping t^\pm , which breaks the Hermiticity of the system. The dotted box indicates a unit cell with two sublattices A and B.

braiding in 1D NH open boundary systems. Going beyond the Bloch band theory, we find an entirely new generic class of topological non-Bloch bands with non-trivial energy braiding, which is generally generated by NHSE. The energies of the Bloch bands do not braid with each other along BZ under periodic boundary condition (PBC). But the one of the non-Bloch bands braid topologically along GBZ under open boundary condition (OBC), such as Hopf link. We propose the non-Bloch winding number and vorticity to characterize the topological energy braiding. The topological phase transition occurs when the gap closes at EPs. Furthermore, the energy braiding is topologically robust against any perturbation without gap closing. Our work paves the way to classify the NH topology for a wide range of 1D NH systems.

Non-Hermitian model. – To explore the complex-energy braiding and the topological properties of the non-Bloch bands, we construct a 1D tight-binding lattice model as shown in Fig.1, whose Hamiltonian in the real space takes

the form:

$$\begin{aligned}
H = & \sum_n \sum_{\sigma \in \{A,B\}} \left(t^- c_{n,\sigma}^\dagger c_{n+1,\sigma} + t^+ c_{n+1,\sigma}^\dagger c_{n,\sigma} \right) \\
& + \frac{m_0}{2} \left(c_{n+1,A}^\dagger c_{n,B} - c_{n+1,B}^\dagger c_{n,A} + H.c. \right) \\
& - \left(im c_{n,A}^\dagger c_{n,B} + H.c. \right), \quad (1)
\end{aligned}$$

here $c_{n,\sigma}^\dagger$ ($c_{n,\sigma}$) is the creation (annihilation) operator of the sublattice $\sigma \in \{A,B\}$ on the n th site. $t^\pm = (t \pm \Delta)/2$ are the non-reciprocal nearest-neighbour hopping in the same sublattice. The Hermiticity of the system is broken by the nonzero parameter Δ . m_0 is the reciprocal nearest-neighbour hopping in different sublattices and m is intracell coupling. The parameters t , Δ , m_0 and m are real.

Non-Hermitian skin effect and the energy braiding of non-Bloch bands. – For concreteness, we illustrate the NH system under PBC firstly. The Bloch Hamiltonian of the periodic boundary system can be written on BZ as:

$$H(k) = t \cos k - i\Delta \sin k + (m + m_0 \sin k)\sigma_y, \quad (2)$$

where σ_y is the Pauli matrix and k is the real-valued Bloch wave vector. The complex eigenenergies $E_\pm(k) = t \cos k - i\Delta \sin k \pm |m + m_0 \sin k|$ are given by the dashed loops in Fig.2(a) - Fig.2(c) for different m with $\Delta = 0.7$ and $m_0 = 0.4$. The PBC energies overlap each other and have a point gap in the complex energy plane.

For NH systems, the physical properties are sensitive to the boundary. The eigenenergies of the open NH system, denoted by the solid curves (red and blue), are different in essence from the PBC eigenenergies. Compared with the PBC eigenenergies, the OBC eigenenergies collapsed and enclosed zero areas in the complex energy plane. In addition, the OBC eigenstates localize at the right side of the open boundary system as shown in the inserts of Fig.2(a)-Fig.2(c). The NHSE and the collapsing of the OBC eigenenergies will certainly result in the non-Bloch band theory in characterizing the NH open boundary system based on the GBZ[6, 52]. The non-Bloch Hamiltonian $H(\beta)$ can be obtained from the Bloch Hamiltonian (Eq.2) by extending the BZ into the GBZ with $\beta = e^{i\tilde{k}}$ and complex-valued non-Bloch wave vector $\tilde{k} = k - i \ln r$. The eigenenergies of the non-Bloch bands take the form $E_\pm(\beta) = \pm m + 0.5(t - \Delta \mp im_0)\beta + 0.5(t + \Delta \pm im_0)\beta^{-1}$.

In contrast to the Bloch band theory, the non-Bloch wave vector has an imaginary part that dictates the localization of the bulk eigenstates and induces the NHSE. The real part of non-Bloch wave vector k , nominated as momentum, is restricted to a period $[0, 2\pi]$. For our system, the GBZ C_β can be determined by the characteristic equation and can be written as $\beta = re^{ik}$ with the amplitude r :

$$r = \sqrt{\left| \frac{t + \Delta + im_0}{t - \Delta - im_0} \right|}. \quad (3)$$

The non-Bloch bands, as described by $\beta(r,k)$ -dependent complex energies, coincide with the eigenenergies of the NH open boundary system, which ensure a good definition of the non-Bloch band theory. Without loss of generality, we can investigate the non-Bloch band structures in the momentum k instead of β . Furthermore, the complex energy of the non-Bloch bands and the momentum k form a three-dimensional (E, k) -space. Then, the separable Bloch band structures of the periodic boundary systems[68] can be generalized into the open boundary systems based on the GBZ. We define a separation $\epsilon_{mn}(k) = E_m(k) - E_n(k)$, which denotes the separation between the non-Bloch bands m and n . A non-Bloch band is "isolated" if the energy does not overlap with that of any other non-Bloch band in the complex energy plane. A non-Bloch band n is "separable" if the separation $\epsilon_{mn}(k) \neq 0$ for all $m \neq n$ and all k . The trajectory of the complex energy along the GBZ can be regarded as a strand of a braid in the three-dimensional (E, k) -space.

Non-Bloch topological invariants. – The ubiquitous twisting and braiding of the two separable non-Bloch bands can be classified by the braid group B_2 . By generalizing the Bloch topological invariants[68, 70], we propose a non-Bloch winding number for the non-Bloch bands on the GBZ as:

$$W = \frac{1}{2\pi i} \oint_{C_\beta} d \ln \det \left[H(\beta) - \frac{1}{2} \text{Tr}(H(\beta)) \right]. \quad (4)$$

This non-Bloch winding number describes how many times the two non-Bloch bands braid along the GBZ, with the sign indicating the handedness of the braiding. Two topologically distinct non-Bloch band structures cannot be continuously deformed into each other without the gap closing, where the non-Bloch winding number changes.

We show the complex eigenenergies of non-Bloch bands along the GBZ in Fig.2(d) - Fig.2(f). The two non-Bloch bands are separable in three-dimensional (E, k) -space, even though they overlap each other in the complex energy plane. What's more remarkable, the separable non-Bloch band structures of Fig.2(d) and Fig.2(f) are topologically distinct. In Fig.2(d), the two non-Bloch bands braid around each other twice along the GBZ with the non-Bloch winding number $W = 2$, which corresponds to a Hopf link phase. By contrast, the non-Bloch bands in Fig.2(f) do not braid around each other with non-Bloch winding number $W = 0$ and correspond to unlink phase. There is a topological phase transition between topologically nontrivial Hopf link and trivial unlink phases at critical m_c , where the two non-Bloch bands touch at EPs as shown in Fig.2(e). The inserts show the PBC energies in (E, k) -space. The PBC energies do not braid each other and have no topological band structures. Therefore, the topological Hopf link phase of the non-Bloch bands is indeed induced by the NHSE and the collapsing

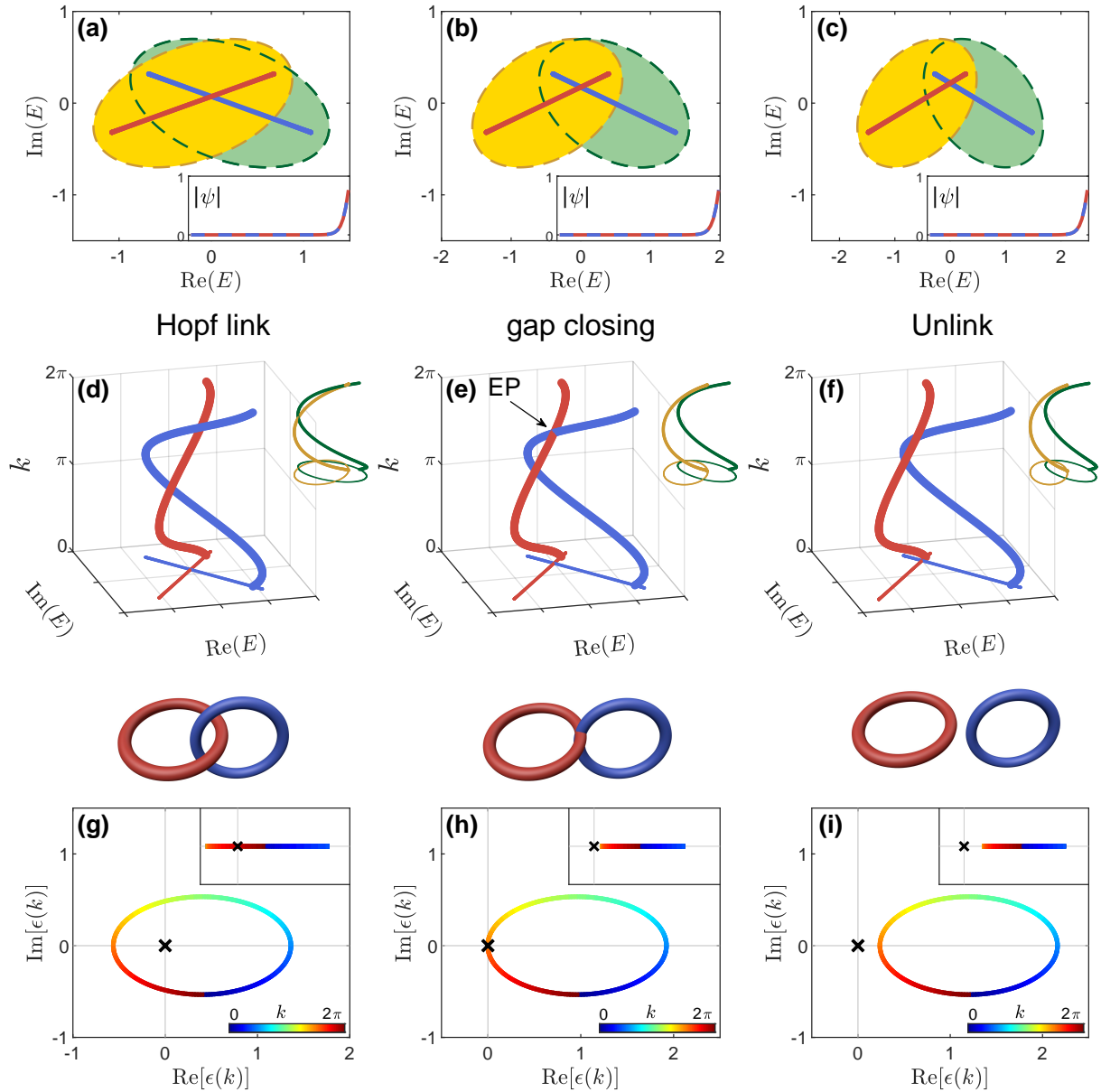


FIG. 2. The complex-energies of the open lattice (solid curves) and periodic lattice (dashed loops) in the complex energy plane for (a) $m = 0.2$, (b) $m = 0.48$ and (c) $m = 0.6$ with $t = 1.0$, $\Delta = 0.7$, $m_0 = 0.4$. The OBC energies enclose zero areas in contrast to the PBC energies, which enclose nonzero areas (yellow and green) in the complex energy plane. The inserts are the average of the eigenstates of the open boundary systems. The NH systems exhibit NHSE for the localization of the eigenstates. (d)-(f) The complex-energies braiding of the non-Bloch bands in the three-dimensional (E, k) -space. The separable non-Bloch bands of (d) and (f) are topologically distinct and correspond to Hopf link and unlink, respectively. (e) The critical case with two non-Bloch bands touching at an EP. The inserts show the Bloch bands without any topological energy braiding. (g) - (i) The separations of the non-Bloch bands along the GBZ. Topological phases transition occurs with separation closing $\epsilon(k_c) = 0$ at EPs. The inserts are the separations of the Bloch bands.

of the OBC energies. Then, we find that the collapsed OBC energies of the non-Bloch bands braid topologically in the momentum space.

To visualize the topological phase transition, we show the separation $\epsilon(k) = \epsilon_{+-}(k)$ of the two non-Bloch bands in the complex energy plane along the GBZ in Fig.2(g) - Fig.2(i). The separation, always nonzero for the separable

non-Bloch bands, encloses the EP for the topologically nontrivial Hopf link phase in Fig.2(g), but does not enclose it for the unlink phase in Fig.2(i). The topological phase transition between topologically distinct phases occurs only when the separation passes through the EP along the GBZ as shown in Fig.2(h). The inserts show the separations of the Bloch bands for periodic boundary

systems, which do not enclose the EP. The two non-Bloch bands intersect at a critical momentum k_c and $m = m_c$ with $\epsilon(k_c) = 0$ as shown in Fig.3(a). The intersection can be determined from the gap closing with $k_c = \frac{3\pi}{2}$ and $m_c = m_0(r^2 + 1)/2r$ for $m > 0$. For $m < 0$ case, the separation is zero at $k_c = \pi/2$ and $m_c = -m_0(r^2 + 1)/2r$.

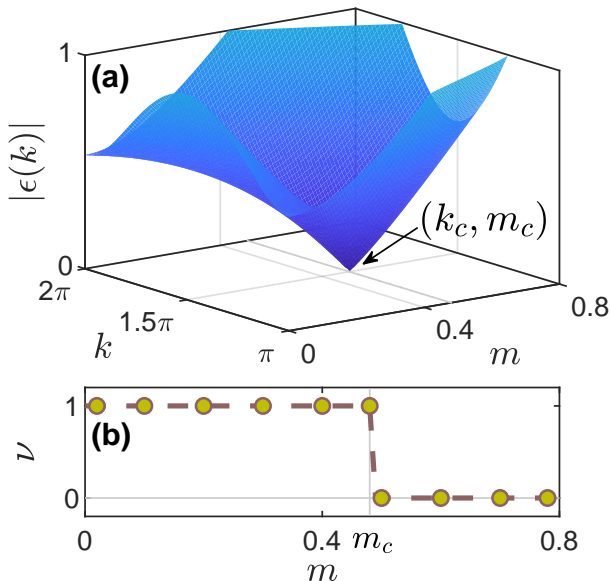


FIG. 3. (a) The absolute value of the separation $\epsilon(k)$ of the non-Bloch bands as a function of m and k along the GBZs. The other parameters are identical to that of Fig.2. As increasing m , the separation has a node with $\epsilon(3\pi/2) = 0$ at a critical value m_c , where the topological phase transition occurs. (b) The non-Bloch vorticity of the two non-Bloch bands as a function of m . The vorticity is 1 for the topological Hopf link phase and 0 for the unlink phase.

The argument of the separation on the GBZ contributes to the topological invariants - non-Bloch vorticity:

$$\nu = \frac{1}{2\pi} \oint_{C_\beta} d \arg [\epsilon(\beta)]. \quad (5)$$

Fig.3(b) shows the non-Bloch vorticity varies with m . The vorticity, which is half of the non-Bloch winding number with $\nu = W/2$, is 1 for the topological Hopf link phase and 0 for the topologically trivial unlink phase. It changes an integer at the topological phase transition between the Hopf link and the unlink phases.

Phase diagram.— In Fig.4 we show a phase diagram with respect to the parameters m and m_0 . The boundary between the separable and isolated phases can be determined with $m = \sqrt{[(t - \Delta)r + (t + \Delta)/r]^2 + (m_0 r + m_0/r)^2}/2$. The separable phase is Hopf link with $m < m_0(r^2 + 1)/2r$ and unlink for other regions. There is an intrinsic difference between phase diagrams of the open and the periodic boundary systems. For periodic boundary system,

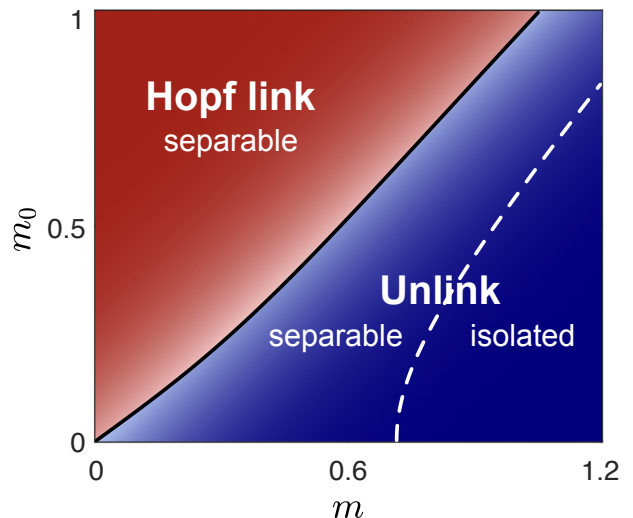


FIG. 4. Phase diagram of the non-Hermitian open boundary system in the $m - m_0$ plane with $t = 1.0$ and $\Delta = 0.7$. The dotted curve denotes the boundary between the phases of separable and isolated. For the separable regions, the solid curve is the boundary between topologically nontrivial Hopf link and the trivial unlink phases.

all the phases are topologically trivial without any non-trivial complex energy braiding. The topological energy braiding of the open boundary system is generated by the NHSE. In addition, the energy braiding of the non-Bloch bands is topologically robust against any perturbation without gap closing. For example, we can introduce a mismatched perturbation δ on the intracell coupling m . Although the GBZ is no longer a circle, the energies of the non-Bloch bands also topologically braid for the Hopf link phase. The perturbation only slightly changes the phase transition point without breaking the energy braiding. The robust properties of the topological energy braiding in the open boundary NH systems ensure the realization in future experiments.

Conclusion.— We have uncovered the topological energy braiding of the non-Bloch bands in a 1D NH open boundary systems. Due to the NHSE, the non-Bloch band structures are topologically different from that of the Bloch bands. In particular, the complex energies of non-Bloch bands braid topologically in momentum space and correspond to the Hopf link, in contrast to the topologically trivial Bloch bands. Furthermore, we have proposed the non-Bloch winding number and vorticity to characterize the topological energy braiding based on the GBZ. The topological distinct phases can not be continuously transformed into each other without the gap closing at exceptional points. The energy braiding of the non-Bloch bands is topologically robust against any perturbation without gap closing. Our work can be extended to investigate other sophisticated knots and links in non-Bloch bands and high dimensionl NH systems, the effects

of the non-Bloch PT symmetry, and so on. We anticipate that our work can pave the way to explore the topological energy braiding of the non-Bloch bands in NH systems.

Acknowledgements. – We thank Z. Wang for fruitful discussions. This work was supported by the National Natural Science Foundation of China (NSFC) under Grant 12174157 and 12074150.

Derivation of the GBZ C_β

According to the Hamiltonian Eq.(1) in the main text, the real space eigen-equation leads to

$$\begin{aligned} & -im\psi_{n,B} + t^- \psi_{n+1,A} + t^+ \psi_{n-1,A} \\ & - \frac{m_0}{2} \psi_{n+1,B} + \frac{m_0}{2} \psi_{n-1,B} = E\psi_{n,A} \\ & im\psi_{n,A} + t^- \psi_{n+1,B} + t^+ \psi_{n-1,B} \\ & + \frac{m_0}{2} \psi_{n+1,A} - \frac{m_0}{2} \psi_{n-1,A} = E\psi_{n,B} \end{aligned} \quad (6)$$

Taking the ansatz that $|\psi\rangle = \sum_j |\psi^{(j)}\rangle$, where j is an independent component index of the wave function. Firstly, omitting the j index and each $|\psi^j\rangle$ takes the exponential form: $(\phi_{n,A}, \phi_{n,B}) = \beta^n (\phi_A, \phi_B)$, which satisfies

$$\begin{aligned} \left(-im - \frac{m_0}{2}\beta + \frac{m_0}{2}\beta^{-1}\right)\phi_B &= (E - t^- \beta - t^+ \beta^{-1})\phi_A \\ \left(im + \frac{m_0}{2}\beta - \frac{m_0}{2}\beta^{-1}\right)\phi_A &= (E - t^- \beta - t^+ \beta^{-1})\phi_B \end{aligned} \quad (7)$$

Then, we have

$$\phi_B = \pm i\phi_A \quad (8)$$

The eigen-equation in both above two cases are a quadratic equation for β . When $\phi_B = i\phi_A$, one can obtain

$$\beta_1\beta_2 = \frac{t + \Delta + im_0}{t - \Delta - im_0} \quad (9)$$

while

$$\beta'_1\beta'_2 = \frac{t + \Delta - im_0}{t - \Delta + im_0} \quad (10)$$

for $\phi_B = -i\phi_A$. The presence of two roots implies that the index of the wave function is $j = 1, 2$. Therefore, restoring the j index, the general solution is written as a linear combination:

$$\begin{aligned} \psi_{n,A} &= \beta_1^n \phi_A^{(1)} + \beta_2^n \phi_A^{(2)} \\ \psi_{n,B} &= \beta_1^n \phi_B^{(1)} + \beta_2^n \phi_B^{(2)} \end{aligned} \quad (11)$$

and $\psi_{n,B} = \pm i\psi_{n,A}$, which should satisfy the boundary

condition:

$$\begin{aligned} & -im\psi_{1,B} + t^- \psi_{2,A} - \frac{m_0}{2} \psi_{2,B} = E\psi_{1,A} \\ & im\psi_{1,A} + t^- \psi_{2,B} + \frac{m_0}{2} \psi_{2,A} = E\psi_{1,B} \\ & -im\psi_{L,B} + t^+ \psi_{L-1,A} + \frac{m_0}{2} \psi_{L-1,B} = E\psi_{L,A} \\ & im\psi_{L,A} + t^+ \psi_{L-1,B} - \frac{m_0}{2} \psi_{L-1,A} = E\psi_{L,B} \end{aligned} \quad (12)$$

For the case of $\psi_{n,B} = i\psi_{n,A}$, the boundary condition is reduced to

$$\begin{aligned} (m - E)\psi_{1,A} + \left(t^- - \frac{im_0}{2}\right)\psi_{2,A} &= 0 \\ (m - E)\psi_{L,A} + \left(t^+ + \frac{im_0}{2}\right)\psi_{L-1,A} &= 0 \end{aligned} \quad (13)$$

Bringing it into the expression of the wave function to eliminate the unknown, we have

$$\beta_1^{L+1} = \beta_2^{L+1} \quad (14)$$

which means $|\beta_1| = |\beta_2|$. Combined with $\beta_1\beta_2 = (t + \Delta + im_0)(t - \Delta - im_0)$, $|\beta_1| = |\beta_2|$ leads to

$$|\beta_j| = r_+ = \sqrt{\left|\frac{t + \Delta + im_0}{t - \Delta - im_0}\right|} \quad (15)$$

By the same method, when $\psi_{n,B} = -i\psi_{n,A}$, we have

$$|\beta'_j| = r_- = \sqrt{\left|\frac{t + \Delta - im_0}{t - \Delta + im_0}\right|} \quad (16)$$

Non-Bloch winding number and the non-Bloch vorticity

The non-Bloch Hamiltonian in terms of β can be written as:

$$H(\beta) = \begin{bmatrix} t^- \beta + t^+ \beta^{-1} & -im - \frac{m_0}{2}(\beta - \beta^{-1}) \\ im + \frac{m_0}{2}(\beta - \beta^{-1}) & t^- \beta + t^+ \beta^{-1} \end{bmatrix}, \quad (17)$$

with the eigenenergies

$$\begin{aligned} E_+(\beta) &= m + \frac{t - \Delta - im_0}{2}\beta + \frac{t + \Delta + im_0}{2}\beta^{-1}, \\ E_-(\beta) &= -m + \frac{t - \Delta + im_0}{2}\beta + \frac{t + \Delta - im_0}{2}\beta^{-1}. \end{aligned} \quad (18)$$

From the non-Bloch Hamiltonian, the non-Bloch wind-

ing number can be simplified:

$$\begin{aligned}
W &= \frac{1}{2\pi i} \oint_{C_\beta} d \ln \det \left[H_\beta - \frac{1}{2} \text{Tr}(H_\beta) \right] \\
&= \frac{1}{2\pi i} \oint_{C_\beta} d \ln \left\{ \left[E_+(\beta) - \frac{1}{2} \text{Tr}(H_\beta) \right] \left[E_-(\beta) - \frac{1}{2} \text{Tr}(H_\beta) \right] \right\} \\
&= \frac{1}{2\pi i} \oint_{C_\beta} d \ln \left\{ \frac{i}{2} [E_+(\beta) - E_-(\beta)] \right\}^2 \\
&= \frac{1}{\pi i} \oint_{C_\beta} d \ln \left\{ \frac{i}{2} |E_+(\beta) - E_-(\beta)| e^{\arg[E_+(\beta) - E_-(\beta)]} \right\} \\
&= \frac{1}{\pi} \oint_{C_\beta} d \arg [E_+(\beta) - E_-(\beta)] \\
&= 2\nu.
\end{aligned} \tag{20}$$

Then, we have the relationship between the two non-Bloch topological invariants: $W = 2\nu$.

The robust energies braiding of non-Bloch bands

Here, we show that the energies braiding of the non-Bloch bands is topologically robust against perturbations for example at intracell coupling m :

$$\begin{aligned}
H &= \sum_n \sum_{\sigma \in \{A, B\}} \left(t^- c_{n, \sigma}^\dagger c_{n+1, \sigma} + t^+ c_{n+1, \sigma}^\dagger c_{n, \sigma} \right) \\
&+ \frac{m_0}{2} \left(c_{n+1, A}^\dagger c_{n, B} - c_{n+1, B}^\dagger c_{n, A} + H.c. \right) \\
&- im c_{n, A}^\dagger c_{n, B} + (im + \delta) c_{n, B}^\dagger c_{n, A}.
\end{aligned} \tag{21}$$

The complex energies braiding of the non-Bloch bands are shown in Fig.5(a)-Fig.5(c) with $\delta = 0.1$. The GBZ is no longer a circle. In Fig.5(a), the complex energies of the non-Bloch bands braid around each other twice along the GBZ, which corresponds to a Hopf link phase. The complex energies in Fig.5(c) do not braid around each other and correspond to unlink phase. There is a topological phase transition between Hopf link and unlink phases at critical $m = 0.46$, where the two non-Bloch bands touch at EPs as shown in Fig.5(b). The separations are shown in Fig.5(d)-Fig.5(e). Therefore, the perturbation δ only changes the phase transition point but not breaks the topological energies braiding of the non-Bloch bands.

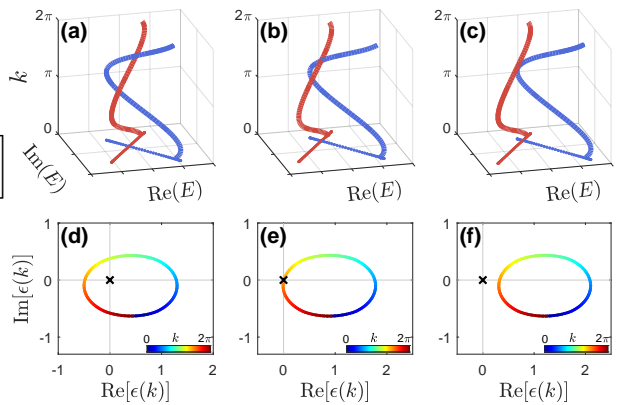


FIG. 5. The complex-energies braiding of the non-Bloch bands in the three dimensional (E, k) -space for (a) $m = 0.2$, (b) $m = 0.46$ and (c) $m = 0.6$ with $t = 1$, $\Delta = 0.7$, $m_0 = 0.4$ and $\delta = 0.1$. The complex energies of the separable non-Bloch bands braid each other along GBZ and robust against δ . (d)-(f) The separations of the non-Bloch bands along the GBZ.

* ypchen@ujs.edu.cn

† yangxs@ujs.edu.cn

- [1] Carl M. Bender and Stefan Boettcher, “Real spectra in non-hermitian hamiltonians having \mathcal{PT} symmetry,” *Phys. Rev. Lett.* **80**, 5243 (1998).
- [2] Carl M Bender, “Making sense of non-hermitian hamiltonians,” *Rep.Prog.Phys* **70**, 947–1018 (2007).
- [3] Ingrid Rotter, “A non-hermitian hamilton operator and the physics of open quantum systems,” *Journal of Physics A* **42**, 153001 (2009).

- [4] Hui Cao and Jan Wiersig, “Dielectric microcavities: Model systems for wave chaos and non-hermitian physics,” *Rev. Mod. Phys.* **87**, 61 (2015).
- [5] Tony E. Lee, “Anomalous edge state in a non-hermitian lattice,” *Phys. Rev. Lett.* **116**, 133903 (2016).
- [6] Shunyu Yao and Zhong Wang, “Edge states and topological invariants of non-hermitian systems,” *Phys. Rev. Lett.* **121**, 086803 (2018).
- [7] Emil J. Bergholtz, Jan Carl Budich, and Flore K. Kunst, “Exceptional topology of non-hermitian systems,” *Rev. Mod. Phys.* **93**, 015005 (2021).
- [8] Simon Malzard, Charles Poli, and Henning Schomerus, “Topologically protected defect states in open photonic systems with non-hermitian charge-conjugation and parity-time symmetry,” *Phys. Rev. Lett.* **115**, 200402 (2015).
- [9] Mingshan Pan, Han Zhao, Pei Miao, Stefano Longhi, and Liang Feng, “Photonic zero mode in a non-hermitian photonic lattice,” *Nat. Commun.* **9**, 1308 (2018).
- [10] Tomoki Ozawa, Hannah M. Price, Alberto Amo, Nathan Goldman, Mohammad Hafezi, Ling Lu, Mikael C. Rechtsman, David Schuster, Jonathan Simon, Oded Zeitlinger, and Iacopo Carusotto, “Topological photonics,” *Rev. Mod. Phys.* **91**, 015006 (2019).
- [11] Hengyun Zhou, Jong Yeon Lee, Shang Liu, and Bo Zhen, “Exceptional surfaces in PT-symmetric non-Hermitian photonic systems,” *Optica* **6**, 190 (2019).
- [12] Lei Xiao, Tianshu Deng, Kunkun Wang, Gaoyan Zhu, Zhong Wang, Wei Yi, and Peng Xue, “Non-hermitian bulk-boundary correspondence in quantum dynamics,” *Nat. Phys.* **16**, 761 (2020).
- [13] Xueyi Zhu, Huaiqiang Wang, Samit Kumar Gupta, Haijun Zhang, Biye Xie, Minghui Lu, and Yanfeng Chen, “Photonic non-hermitian skin effect and non-bloch bulk-boundary correspondence,” *Phys. Rev. Research* **2**, 013280 (2020).
- [14] Kunkun Wang, Lei Xiao, Jan Carl Budich, Wei Yi, and Peng Xue, “Simulating exceptional non-hermitian metals with single-photon interferometry,” *Phys. Rev. Lett.* **127**,

- 026404 (2021).
- [15] Tony E. Lee and Ching-Kit Chan, “Heralded magnetism in non-hermitian atomic systems,” *Phys. Rev. X* **4**, 041001 (2014).
- [16] Yong Xu, Sheng-Tao Wang, and L.-M. Duan, “Weyl exceptional rings in a three-dimensional dissipative cold atomic gas,” *Phys. Rev. Lett.* **118**, 045701 (2017).
- [17] Rong Wen, Chang-Ling Zou, Xinyu Zhu, Peng Chen, Z. Y. Ou, J. F. Chen, and Weiping Zhang, “Non-hermitian magnon-photon interference in an atomic ensemble,” *Phys. Rev. Lett.* **122**, 253602 (2019).
- [18] Peng He, Jia-Hao Fu, Dan-Wei Zhang, and Shi-Liang Zhu, “Double exceptional links in a three-dimensional dissipative cold atomic gas,” *Phys. Rev. A* **102**, 023308 (2020).
- [19] Lei Pan, Xin Chen, Yu Chen, and Hui Zhai, “Non-hermitian linear response theory,” *Nat. Phys* **16**, 767 (2020).
- [20] Zhaoli Dong Haowei Li Hang Li Bryce Gadway Wei Yi Qian Liang, Dizhou Xie and Bo Yan, “Observation of non-hermitian skin effect and topology in ultracold atoms,” [arXiv:2201.09478](https://arxiv.org/abs/2201.09478) (2022).
- [21] Mudi Wang, Liping Ye, J. Christensen, and Zhengyou Liu, “Valley physics in non-hermitian artificial acoustic boron nitride,” *Phys. Rev. Lett.* **120**, 246601 (2018).
- [22] Chen Shen, Junfei Li, Xiuyuan Peng, and Steven A. Cummer, “Synthetic exceptional points and unidirectional zero reflection in non-hermitian acoustic systems,” *Phys. Rev. Materials* **2**, 125203 (2018).
- [23] He Gao, Haoran Xue, Zhongming Gu, Tuo Liu, Jie Zhu, and Baile Zhang, “Non-hermitian route to higher-order topology in an acoustic crystal,” *Nat. Commun.* **12**, 1888 (2021).
- [24] Li Zhang, Yihao Yang, Yong Ge, Yi-Jun Guan, Qiaolu Chen, Qinghui Yan, Fujia Chen, Rui Xi, Yuanzhen Li, Ding Jia, Shou-Qi Yuan, Hong-Xiang Sun, Hongsheng Chen, and Baile Zhang, “Acoustic non-hermitian skin effect from twisted winding topology,” *Nat. Commun.* **12**, 6297 (2021).
- [25] Xiujian Zhang, Yuan Tian, Jian-Hua Jiang, Ming-Hui Lu, and Yan-Feng Chen, “Observation of higher-order non-hermitian skin effect,” *Nat. Commun.* **12**, 5377 (2021).
- [26] Mário G. Silveirinha, “Topological theory of non-hermitian photonic systems,” *Phys. Rev. B* **99**, 125155 (2019).
- [27] Xingping Zhou, Jing Wu, and Yongfeng Wu, “Topological corner states in non-Hermitian photonic crystals,” *Opt. Commun.* **466**, 125653 (2020).
- [28] Linhu Li, Ching Hua Lee, and Jiangbin Gong, “Topological switch for non-hermitian skin effect in cold-atom systems with loss,” *Phys. Rev. Lett.* **124**, 250402 (2020).
- [29] Weiwei Zhu, Xinsheng Fang, Dongting Li, Yong Sun, Yong Li, Yun Jing, and Hong Chen, “Simultaneous observation of a topological edge state and exceptional point in an open and non-hermitian acoustic system,” *Phys. Rev. Lett.* **121**, 124501 (2018).
- [30] Zhongming Gu, He Gao, Tuo Liu, Shanjun Liang, Shuwei An, Yong Li, and Jie Zhu, “Topologically protected exceptional point with local non-hermitian modulation in an acoustic crystal,” *Phys. Rev. Applied* **15**, 014025 (2021).
- [31] Hengyun Zhou, Chao Peng, Yoseob Yoon, Chia Wei Hsu, Keith A. Nelson, Liang Fu, John D. Joannopoulos, Marin Soljačić, and Bo Zhen, “Observation of bulk Fermi arc and polarization half charge from paired exceptional points,” *Science* **359**, 1009–1012 (2018).
- [32] Mohammad-Ali Miri and Andrea Al, “Exceptional points in optics and photonics,” *Science* **363**, eaar7709 (2019).
- [33] Choloong Hahn, Youngsun Choi, Jae Woong Yoon, Seok Ho Song, Cha Hwan Oh, and Pierre Berini, “Observation of exceptional points in reconfigurable non-hermitian vector-field holographic lattices,” *Nat. Commun.* **7**, 12201 (2016).
- [34] Kohei Kawabata, Takumi Bessho, and Masatoshi Sato, “Classification of exceptional points and non-hermitian topological semimetals,” *Phys. Rev. Lett.* **123**, 066405 (2019).
- [35] W. B. Rui, Y. X. Zhao, and Andreas P. Schnyder, “Topology and exceptional points of massive dirac models with generic non-hermitian perturbations,” *Phys. Rev. B* **99**, 241110 (2019).
- [36] Kazuki Yokomizo and Shuichi Murakami, “Topological semimetal phase with exceptional points in one-dimensional non-hermitian systems,” *Phys. Rev. Research* **2**, 043045 (2020).
- [37] Xizheng Zhang and Jiangbin Gong, “Non-hermitian floquet topological phases: Exceptional points, coalescent edge modes, and the skin effect,” *Phys. Rev. B* **101**, 045415 (2020).
- [38] Lei Xiao, Tianshu Deng, Kunkun Wang, Zhong Wang, Wei Yi, and Peng Xue, “Observation of non-bloch parity-time symmetry and exceptional points,” *Phys. Rev. Lett.* **126**, 230402 (2021).
- [39] Nobuyuki Okuma, Kohei Kawabata, Ken Shiozaki, and Masatoshi Sato, “Topological origin of non-hermitian skin effects,” *Phys. Rev. Lett.* **124**, 086801 (2020).
- [40] Fei Song, Shunyu Yao, and Zhong Wang, “Non-hermitian skin effect and chiral damping in open quantum systems,” *Phys. Rev. Lett.* **123**, 170401 (2019).
- [41] Stefano Longhi, “Probing non-hermitian skin effect and non-bloch phase transitions,” *Phys. Rev. Research* **1**, 023013 (2019).
- [42] Hui Jiang, Li-Jun Lang, Chao Yang, Shi-Liang Zhu, and Shu Chen, “Interplay of non-hermitian skin effects and anderson localization in nonreciprocal quasiperiodic lattices,” *Phys. Rev. B* **100**, 054301 (2019).
- [43] Ching Hua Lee, Linhu Li, and Jiangbin Gong, “Hybrid higher-order skin-topological modes in nonreciprocal systems,” *Phys. Rev. Lett.* **123**, 016805 (2019).
- [44] Linhu Li, Ching Hua Lee, Sen Mu, and Jiangbin Gong, “Critical non-hermitian skin effect,” *Nat. Commun.* **11**, 5491 (2020).
- [45] Chun-Hui Liu, Kai Zhang, Zhesen Yang, and Shu Chen, “Helical damping and dynamical critical skin effect in open quantum systems,” *Phys. Rev. Research* **2**, 043167 (2020).
- [46] Tobias Hofmann, Tobias Helbig, Frank Schindler, Nora Salgo, Marta Brzezińska, Martin Greiter, Tobias Kiessling, David Wolf, Achim Vollhardt, Anton Kabaši, Ching Hua Lee, Ante Bilušić, Ronny Thomale, and Titus Neupert, “Reciprocal skin effect and its realization in a topoelectrical circuit,” *Phys. Rev. Research* **2**, 023265 (2020).
- [47] Yifei Yi and Zhesen Yang, “Non-hermitian skin modes induced by on-site dissipations and chiral tunneling effect,” *Phys. Rev. Lett.* **125**, 186802 (2020).
- [48] Shuo Liu, Ruiwen Shao, Shaojie Ma, Lei Zhang, Oubo

- You, Haotian Wu, Yuan Jiang Xiang, Tie Jun Cui, and Shuang Zhang, “Non-hermitian skin effect in a non-hermitian electrical circuit,” *Research* **2021**, 5608038 (2021).
- [49] Cui-Xian Guo, Chun-Hui Liu, Xiao-Ming Zhao, Yanxia Liu, and Shu Chen, “Exact solution of non-hermitian systems with generalized boundary conditions: Size-dependent boundary effect and fragility of the skin effect,” *Phys. Rev. Lett.* **127**, 116801 (2021).
- [50] Taiki Haga, Masaya Nakagawa, Ryusuke Hamazaki, and Masahito Ueda, “Liouvillian skin effect: Slowing down of relaxation processes without gap closing,” *Phys. Rev. Lett.* **127**, 070402 (2021).
- [51] Wen-Tan Xue, Yu-Min Hu, Fei Song, and Zhong Wang, “Non-hermitian edge burst,” *Phys. Rev. Lett.* **128**, 120401 (2022).
- [52] Kazuki Yokomizo and Shuichi Murakami, “Non-bloch band theory of non-hermitian systems,” *Phys. Rev. Lett.* **123**, 066404 (2019).
- [53] Flore K. Kunst, Elisabet Edvardsson, Jan Carl Budich, and Emil J. Bergholtz, “Biorthogonal bulk-boundary correspondence in non-hermitian systems,” *Phys. Rev. Lett.* **121**, 026808 (2018).
- [54] L. Jin and Z. Song, “Bulk-boundary correspondence in a non-hermitian system in one dimension with chiral inversion symmetry,” *Phys. Rev. B* **99**, 081103 (2019).
- [55] Ananya Ghatak, Martin Brandenbourger, Jasper van Wezel, and Corentin Coulais, “Observation of non-hermitian topology and its bulk-edge correspondence in an active mechanical metamaterial,” *PNAS* **117**, 29561 (2020).
- [56] Huaiqiang Wang, Jiawei Ruan, and Haijun Zhang, “Non-hermitian nodal-line semimetals with an anomalous bulk-boundary correspondence,” *Phys. Rev. B* **99**, 075130 (2019).
- [57] Elisabet Edvardsson, Flore K. Kunst, and Emil J. Bergholtz, “Non-hermitian extensions of higher-order topological phases and their biorthogonal bulk-boundary correspondence,” *Phys. Rev. B* **99**, 081302 (2019).
- [58] T. Helbig, T. Hofmann, S. Imhof, M. Abdelghany, T. Kiessling, L. W. Molenkamp, C. H. Lee, A. Szameit, M. Greiter, and R. Thomale, “Generalized bulk-boundary correspondence in non-hermitian topoelectrical circuits,” *Nat. Phys* **16**, 747 (2020).
- [59] S. Longhi, “Non-bloch-band collapse and chiral zener tunneling,” *Phys. Rev. Lett.* **124**, 066602 (2020).
- [60] Xiao-Ran Wang, Cui-Xian Guo, and Su-Peng Kou, “Defective edge states and number-anomalous bulk-boundary correspondence in non-hermitian topological systems,” *Phys. Rev. B* **101**, 121116 (2020).
- [61] Zhicheng Zhang, Zhesen Yang, and Jiangping Hu, “Bulk-boundary correspondence in non-hermitian hopf-link exceptional line semimetals,” *Phys. Rev. B* **102**, 045412 (2020).
- [62] Yang Cao, Yang Li, and Xiaosen Yang, “Non-hermitian bulk-boundary correspondence in a periodically driven system,” *Phys. Rev. B* **103**, 075126 (2021).
- [63] Heinrich-Gregor Zirnstein, Gil Refael, and Bernd Rosenow, “Bulk-boundary correspondence for non-hermitian hamiltonians via green functions,” *Phys. Rev. Lett.* **126**, 216407 (2021).
- [64] Fei Song, Shunyu Yao, and Zhong Wang, “Non-hermitian topological invariants in real space,” *Phys. Rev. Lett.* **123**, 246801 (2019).
- [65] Shunyu Yao, Fei Song, and Zhong Wang, “Non-hermitian chern bands,” *Phys. Rev. Lett.* **121**, 136802 (2018).
- [66] Mark R. Hirsbrunner, Timothy M. Philip, and Matthew J. Gilbert, “Topology and observables of the non-hermitian chern insulator,” *Phys. Rev. B* **100**, 081104 (2019).
- [67] Wojciech Brzezicki and Timo Hyart, “Hidden chern number in one-dimensional non-hermitian chiral-symmetric systems,” *Phys. Rev. B* **100**, 161105 (2019).
- [68] Huitao Shen, Bo Zhen, and Liang Fu, “Topological band theory for non-hermitian hamiltonians,” *Phys. Rev. Lett.* **120**, 146402 (2018).
- [69] Charles C. Wojcik, Kai Wang, Avik Dutt, Janet Zhong, and Shanhui Fan, “Eigenvalue topology of non-hermitian band structures in two and three dimensions,” (2021), 10.48550/arxiv.2111.09977.
- [70] Kai Wang, Avik Dutt, Charles C. Wojcik, and Shanhui Fan, “Topological complex-energy braiding of non-Hermitian bands,” *Nature* **598**, 59 (2021).
- [71] Haiping Hu and Erhai Zhao, “Knots and Non-Hermitian Bloch Bands,” *Phys. Rev. Lett.* **126**, 010401 (2021).
- [72] Yefei Yu, Li-Wei Yu, Wengang Zhang, Huili Zhang, Xiaolong Ouyang, Yanqing Liu, Dong-Ling Deng, and L. M. Duan, “Experimental unsupervised learning of non-hermitian knotted phases with solid-state spins,” (2021), 10.48550/arxiv.2112.13785.
- [73] Louis H Kauffman, *Knots and Physics*, Vol. 53 (World scientific, 2013).
- [74] Charles C. Wojcik, Xiao-Qi Sun, Tomá š Bzdušek, and Shanhui Fan, “Homotopy characterization of non-hermitian hamiltonians,” *Phys. Rev. B* **101**, 205417 (2020).